Speciation and Persistence of Dimethoate in the Aquatic Environment: Characterization in Terms of a Rate Model that Takes Into Account Hydrolysis, Photolysis, Microbial Degradation and Adsorption of the Pesticide by Colloidal and Sediment Particles

Mark F. Zaranyika* and Justin Mlilo

Chemistry Department, University of Zimbabwe, P.O. Box MP167, Mount Pleasant, Harare, Zimbabwe.

Received 20 October 2013, revised 29 August 2014, accepted 6 November 2014.

ABSTRACT

The kinetics of the degradation of dimethoate in an aquatic microcosm ecosystem, and a distilled water control, charged with the pesticide was studied over a period of 90 days. The concentration of dimethoate was monitored in the distilled water control, as well as the water phase and sediment phase of the experiment. The loss of the pesticide after a given time period was calculated and plotted as a function of time. Biphasic linear rates of dimethoate degradation were observed for both the water phase (3.12 and 0.358 μg mL^{-1} day^{-1}, respectively) and the sediment phase (108 and 1.03 μg g^{-1} day^{-1}, respectively) in the experimental microcosm, as well as the distilled water control (0.694 and 0.0388 μg mL^{-1} day^{-1}, respectively). The linear rates of degradation in distilled water are attributed to hydrolysis and photochemical degradation. The biphasic linear rates of degradation in the experimental microcosm are attributed to microbial degradation of pesticide adsorbed by sediment or colloidal particles, and an enzymatic kinetics model is presented to account for the observed kinetics. The factors that affect the rates of degradation, possible dimethoate pollution remediation strategies, and characterization of the different speciation forms in terms of rates of degradation and apparent adsorption/desorption thermodynamic properties, are discussed.

KEYWORDS

Dimethoate, degradation rates, pesticide, adsorption/desorption kinetics, chemisorption.

1. Introduction

Dimethoate, [*O,O*-dimethyl *S*-[2-(methylamino)-2-oxoethyl] phosphorodithioate, CAS Registry No. 60-51-5], is an organophosphate insecticide marketed under various trade names. It is a systematic insecticide used for the control of a wide variety of insect pests (Acari, Aphididae, Aleyrodidae, Coccidae, Coleoptera, Collembola, Diptera, Lepidoptera, Pseudococcidae and Thysanoptera) in cereals, citrus, coffee, cotton, grapes, olives, pastures, beetroot, potatoes, pulses, tea, tobacco and vegetables. It is also used for the control of flies on animals and in animal houses.[1]

Dimethoate is moderately toxic to mammals and is classified as a possible human carcinogen by the US EPA, based on occurrence of tumours in exposed mice.[2] Like other organophosphates, dimethoate is an acetyl cholinesterase inhibitor, and works primarily as a nerve poison.[3–10] It is slightly toxic to estuarine and marine invertebrates, highly toxic to freshwater fish and invertebrates, and very toxic to birds.[1,2] In the case of fish, the effect of exposure to dimethoate is reflected in the uncoordinated abnormal behaviour of the fish soon after exposure. LC_{50} values of 1.84, 1.78, 1.68 and 1.61 mg L^{-1} for 24, 48, 72 and 96 hours of exposure to dimethoate were reported for fingerlings of the common carp, *Cypricus carpia*, exposed to the pesticide.[9] Heavy contamination of aquatic ecosystems by the pesticide can lead to mass mortality of fish and other organisms.[11]

* To whom correspondence should be addressed. E-mail: zaranyika@science.uz.ac.zw

Dimethoate has a vapour pressure of 1.1×10^{-3} Pa at 25 °C.[1] Its solubility in water at 21 °C is 25 g L^{-1}. Reported log values of the octanol-water partition coefficients are 0.78 and 0.79, respectively.[1] Dimethoate is lost from the soil through leaching, evaporation and biodegradation. Its half-life in soil ranges from 4 to 16 days.[8] Dimethoate is relatively stable in aqueous media from pH 2 to 7.5. It is slowly hydrolyzed in aqueous acidic solution (pH 3–6), but is rapidly hydrolyzed in alkaline solutions.[12] Reported half-lives for dimethoate in raw water range from 18 hours to 8 weeks.[8] It hydrolyzes in plants and animals to *O,O*-dimethyl dithiophosphoric acid.

The traditional approach to studying the persistence of pesticides in the environment involves spiking the pesticide into an appropriate compartment of the environment, followed by periodic sampling to determine the amount of pesticide remaining in the medium. The concentration of pesticide remaining at any given time is then plotted as a function of time, to give the persistence curve. In most cases, the persistence curve resembles a first-order decay curve. The persistence of pesticides in the environment is therefore usually expressed in terms of the half-lives of the pesticides in the environment, on the assumption that the persistence curves conform to pseudo-first-order kinetics. Half-life persistence data reported for dimethoate in the literature are highly variable (see Table 1), whereas in true first-order kinetics, a constant value should be obtained for the half-life, irrespective of the actual environmental conditions prevailing.

Table 1 Persistence data for dimethoate reported in the literature.

Environment	Degradation mechanism	Persistence		Ref.
		Degradation/%	Half-life/days	
Soil, drought conditions	Biological		4	13
Soil, moderate rainfall	Biological		2–1/2	13
Soil		(i) 60 (after 4 days)		
		(ii) 80 (after 54 days)		14
Raw water			1.5–56	8
Water at 25 °C	Hydrolysis		30	7
Sterile water at pH 5	Hydrolysis		156	7
Sterile water at pH 7	Hydrolysis		68	7
Sterile water at pH 9	Hydrolysis		4.4	7
Soil, aerobic	Microbial [a]		2.2	2
Soil, anaerobic	Microbial [a]		22	2

[a]Microbially mediated hydrolysis.

Major processes leading to the degradation of pesticides in the environment include hydrolysis, photolysis and microbial action. In addition, pesticides are known to undergo adsorption onto colloidal, sediment and soil particles. Models of the persistence of pesticides should ideally take these factors into account, if they are to have predictive value.[12] Therefore, it is apparent that more studies are required to elucidate further the kinetics of the degradation of pesticides in the aquatic environment.

Zaranyika and co-workers[15–18] have studied the degradation kinetics of several pesticides in aquatic microcosm experiments simulating real environmental variables. Pesticide spiking, sample collection and analysis were done according to the conventional approach described above. The loss in the pesticide after a given time period is monitored and the instantaneous loss plotted as a function of time. Pesticides studied include organophosphates (glyphosate, fenamiphos, chlorpyrifos and pirimiphos-methyl),[15,16] organochlorines (endosulfan I and II),[17] and the bipyrimidium herbicide, paraquat.[18] In all cases, plots with two linear portions were obtained for the water and sediment phases of the experiment. The results were explained in terms of a steady-state enzymatic kinetics model which takes into account microbial degradation and adsorption/desorption of the pesticide by colloidal and sediment particles.

In this paper we report the results of similar semi-field experiments carried out in order to determine whether the degradation of dimethoate in the aquatic environment can be interpreted in terms of the proposed enzymatic kinetics model. The experiments were conducted with dam water and sediment contained in plastic drums covered with clear perforated plastic and exposed to sunlight. The rate of degradation of the pesticide was monitored in the water as well as in the sediment phases of the experiment.

2. Experimental

2.1. Equipment

A microprocessor-controlled Perkin Elmer Autosystem gas chromatograph, equipped with a built-in autosampler, a split/splitless injector, and a nitrogen phosphorus detector (NPD) (Perkin Elmer, Norwalk, CT, USA), was used in conjunction with a BPX-5- 95 % phenyl polydiphenylene-silicone capillary column 30 m × 0.25 mm id, film thickness 0.25 μm (SGE Analytical Science, Melbourne, Australia) to analyze the extracted samples. Also used were two plastic tanks of capacity 200 L each; 3.7 mL Pyrex glass sample vials with hollow caps and Teflon-lined septa (Supelco SA, Switzerland); a Buchi rotary evaporator Model R-124 (Buchi Labortechnik AG, Switzerland) equipped with a water bath was used to concentrate the sample extracts to near dryness, and a Stuart Scientific model SF1 mechanical flask shaker (Stuart Scientific, Redhill, UK).

2.2. Materials

The following solvents were used: pesticide residue analysis grade diethyl ether, ethyl acetate, hexane and acetone (Fischer Scientific, Loughorough, U.K.). Other materials used include glass wool, Florisil (60–100 mesh, [Fluka Chemie AG, Switzerland]); anhydrous sodium sulfate (99.8 % purity, Acros Organics, New Jersey, USA); Whatman 541 filter paper; double-distilled water; dam water and sediment collected from Kutsaga Dam on the Hunyani River near the Tobacco Research Board Kutsaga Research Station, Harare, Zimbabwe; high-purity nitrogen carrier gas; dimethoate reference standard (99.5% pure, supplied by Dr. Ehrenstnfer, D86 199, Ausberg, Germany); Rogor (containing 400 g L^{-1} dimethoate) (supplied by Agricura (Pvt) Ltd., Zimbabwe).

2.3. Procedure

The procedure followed was described previously.[16] Volumes of 100 L each of Kutsaga Dam and distilled water were charged into two separate 200 L tanks and the levels were marked. About 1.93 kg of sediment was added into the tank containing dam water. Equal amounts (37.25 mL) of Rogor were added to each of the tanks to give a final concentration of dimethoate of 149.0 μg mL^{-1}. The contents were thoroughly mixed. Samples were taken immediately after the system had settled. The tanks were covered with transparent perforated polyethylene and left exposed to sunlight on the roof of the Pesticide Analysis Laboratory Building, Kutsaga Research Station. Thereafter, samples of water and sediment were collected periodically for a period of 90 days, each time compensating for the evaporation that occurred 24 hours prior to sampling. Water and sediment samples were taken without disturbing the system. The new level was marked after each sampling, then the system was stirred and left to settle. Once collected, all samples were stored in the freezer in plastic bottles with screw caps until required for analysis. All the samples were thawed and mixed thoroughly prior to analysis.

2.4. Extraction, Cleanup and Concentration

Water samples were analyzed by GC-NPD with a BPX-5, phenyl-polydiphenylene silicon capillary column following liquid–liquid extraction.[19,20] Water samples were analyzed in

duplicate. A volume of 100 mL of water samples were extracted 3 times with 50 mL portions of diethyl ether using a separatory funnel, and collected over anhydrous sodium sulphate. The combined extracts were concentrated to near dryness using the rotary evaporator with the water bath maintained at 40 °C, and then re-dissolved in 2.0 mL acetone for subsequent clean-up prior to analysis by GC-NPD.

Sediment samples were analyzed following solvent extraction.[19] Sediment samples were extracted after the excess water in the sample had been removed by suction from a Buchner funnel through a Whatman No. 1 filter paper, and then air-dried for three hours. The moisture content of the suction and air-dried sediment samples was determined after thoroughly mixing the sample. About 20 g of accurately weighed dried sediment sample was placed in a 250 mL flask, and 100 mL of acetone were added and the flask stoppered. The mixture was then shaken on the mechanical shaker for 30 min, then filtered through anhydrous sodium sulphate. The sample was then quantitatively transferred to the rotary evaporator maintained at 40 °C, and the crude extract was concentrated to near dryness and then re-dissolved in 2 mL acetone for subsequent clean-up prior to GC-NPD analysis.

For clean-up the concentrated extract was transferred to a chromatographic column plugged with glass wool and containing 5 g of Florisil and 1 g of anhydrous Na_2SO_4 pre-cleaned by eluting with 10% diethyl ether in hexane. Care was taken not to let the column run dry. The column was then eluted twice by using 100 mL each of 5 % diethyl ether in hexane and 10 % diethyl ether in hexane. The two fractions were combined and concentrated to near dryness and then re-dissolved in 2 mL acetone for subsequent GC-NPD analysis.[21]

2.5. Gas Chromatography

The gas chromatographic conditions employed are given in Table 2. One microlitre of the concentrated extract was injected each time. Dimethoate eluted at 1.91 minutes in the GC-NPD chromatogram, see Fig. 1. Quantification was done by the external standard technique. Preliminary studies with the spiked sediment and lake water samples showed the average extraction efficiency to be 80 ± 1 % and 84 ± 2 % when sediment samples and lake water samples spiked with 20 ng g^{-1} and 5 ng g^{-1} dimethoate, respectively, were extracted and determined as described above. Dimethoate was not detected when blank determinations were done on the sediment and dam water samples. Figure 2 shows the persistence curves of dimethoate obtained for distilled water, Kutsaga Dam water and Kutsaga Dam sediment. The loss in dimethoate after a given time period, t, in days, i.e. C_t–C_o, was calculated and plotted as a function of t in Fig. 3. The slopes of the linear portions of the curves in Fig. 3 give the respective rates of degradation, and these are summarized in Table 3.

Table 2 Gas chromatographic conditions employed.

GC compartment	Parameter	Setting
Column	Initial temperature	195 °C
	Initial hold time	2.0 min
	Final temperature	235 °C
	Temperature programme	10 °C min^{-1}
	Final hold time	9.0 min
	N_2 carrier gas flow rate	5.2 mL min^{-1}
Injector	Temperature	230 °C
	Mode	Splitless
Detector	Type	NPD
	Temperature	300 °C
	Range	1
	Auto zero	On
	Time constant	200
Detector gas flows	Air	179.0 mL min^{-1}
	Hydrogen	4.4 mL min^{-1}

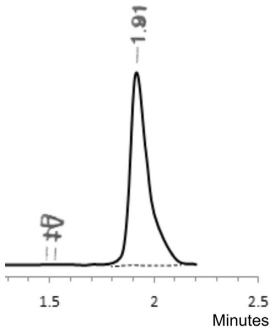

Figure 1 Typical chromatogram for the sediment sample collected on day 9 showing the retention time for dimethoate at 1.91 minutes.

3. Results and Discussion

A heavy green algal growth developed in the dam water plus sediment experiment after 6 days. The algal growth disappeared after 64 days. No algal growth was observed in the distilled water control. Material balance calculations, shown in Table 4, show that of the 14.9 g of dimethoate charged into the experimental microcosm, 2.71 g (18.2 %) was adsorbed by the sediment, while 12.03 g (80.7%) remained in the water phase of the experiment, and the balance of 0.16 g (1.07 %) are presumed to be adsorbed onto the walls of the container. In the distilled water control, 15.23 g (102.2 %) were detected in the water phase, suggesting minimal adsorption by the walls of the plastic tank.

3.1. Rates of Degradation in Distilled Water

Figure 2(a) shows that the losses due to degradation were 81.6 % and 6.4 %, respectively in the lake-water-plus-sediment experiment and distilled water control after 90 days. These data

Table 3 Rates of degradation (μg g^{-1} day^{-1}) of the different speciation forms of dimethoate in the sediment and water phases of the river-water-and-sediment experiment.

Phase	Speciation form [a]	Rate/μg g^{-1} day^{-1}	Persistence/days	Total pesticide/g [b]
Water	D_f	3.12	25	7.80
	$D(C_1)_n$	0.358	>90 (118)	4.24
Sediment	$D(S)_z$	108	9	1.87
	$D(C_1)_m$	1.03	>90 (422)	0.84

[a] Speciation form: D_f = free pesticide in solution; $D(C_1)_n$ = colloidal particle adsorbed pesticide in solution; $D(S)_z$ = sediment particle adsorbed pesticide; $D(C)_m$ = colloidal particle adsorbed pesticide in sediment pore water.
[b] Mass of phase = 100 000 g (water phase) and 1930 g (sediment phase).

Table 4 Material balance calculations: initial and final distribution of dimethoate in the microcosm.

Phase	Initial analysis/μg g^{-1}	Total pesticide/g	Final analysis/μg g^{-1}	Total pesticide/g
Dam water and sediment experiment				
Water	120.3	12.03	20.08	2.08
Sediment	1404	2.71	362	0.699
Container [a]		0.16		0.16
Deg. loss [b]				12.0
Total		14.9		14.9
Distilled water control				
Water	152.3	15.23	142.6	14.26
Container [a]		–		–
Deg. loss [b]				0.97
Total		15.2		15.2

[a] Adsorbed to walls of the container; no change assumed during period of the experiment.
[b] Loss due to degradation.

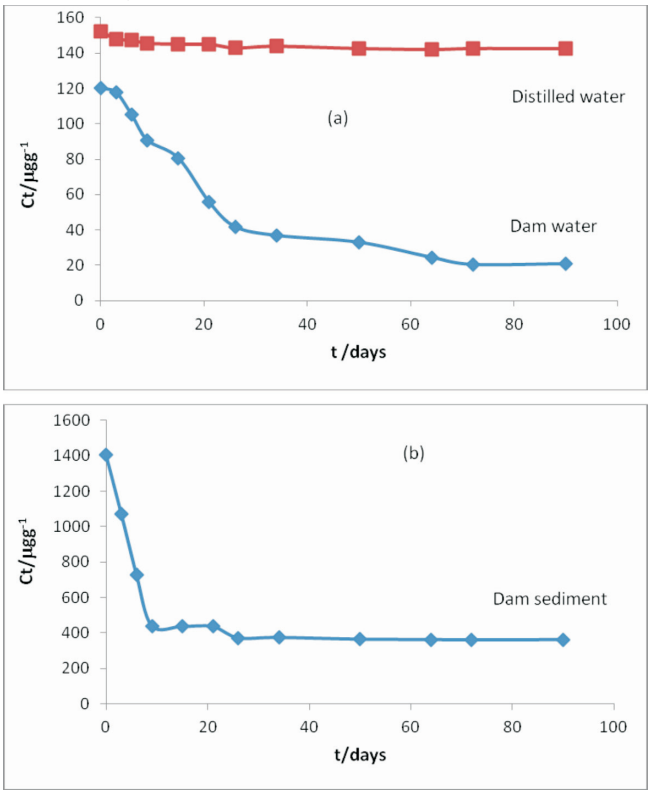

Figure 2 Dimethoate persistence in distilled water and Kutsaga Dam water (**a**), and in Kutsaga Dam sediment (**b**).

suggest that chemical degradation and photodegradation are minor routes for the degradation of dimethoate in the aquatic environment. Figure 3(a) shows that degradation of dimethoate in distilled water proceeds *via* an initial fast rate of 0.694 μg mL^{-1} day^{-1} during the first 9 days, followed by a slower rate of 0.0388 μg mL^{-1} day^{-1} for the rest of the study period.

These rates are only 22 % and 1.2 % of the rate of degradation of 3.12 μg mL^{-1} observed for the water phase of the microcosm experiment in Fig. 3(b). We attribute the initial fast rate in distilled water to hydrolysis, which we assume proceeds *via* an activated transition state complex, DM-H_2O^+, according to the steps in Table 5. It can be shown that:

$$\frac{dP}{dt} = \left(\frac{k_1 k_h}{k_{-1} + k_h}\right)[D]_t = k_h'[D]_t \quad (1)$$

where k_h' is the apparent hydrolysis constant, and $[D]_t$ is the concentration of dimethoate in the system at time t.

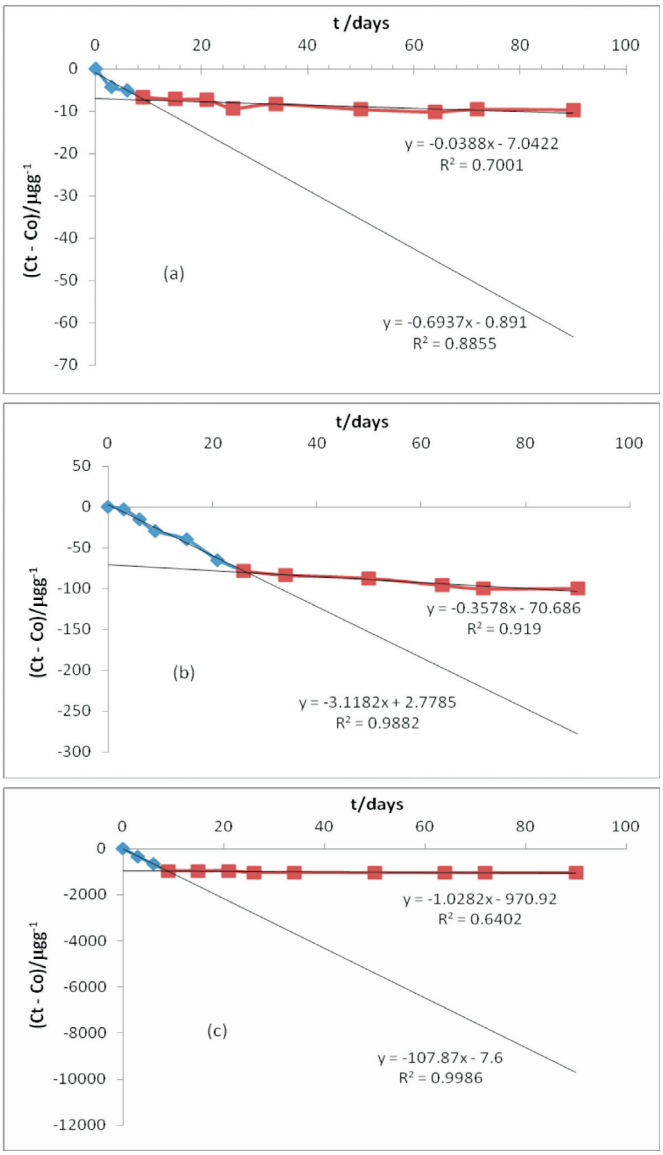

Figure 3 Dimethoate degradation rates in (**a**) distilled water, (**b**) Kutsaga Dam water and (**c**) Kutsaga Dam sediment.

As hydrolysis involves molecules of the solvent, it is expected to be activation energy controlled rather than diffusion controlled. Hence, in the absence of an external source of energy, the rate of hydrolysis is expected to be very slow, consistent with the value of 0.694 μg mL^{-1} day^{-1} observed during the first 9 days.

Table 5 Steps in the hydrolysis of dimethoate (D).

Step	Reaction	Rate constant	
1	$D + H_2O \rightarrow D\text{-}H_2O^{\dagger}$	k_1	Formation of activated complex
2	$D\text{-}H_2O^{\dagger} \rightarrow D + H_2O$	k_{-1}	Reverse reaction
3	$(D\text{-}H_2O)^{\dagger} \rightarrow P$	k_h	Hydrolysis (P = products).

Dimethoate has been reported to be relatively stable in water under acidic conditions, while it hydrolyzes rapidly under alkaline conditions to methylamine, thioglycolic acid and thiophosphate.[22] The fact that the hydrolysis of dimethoate in the distilled water control ceases after 9 days is probably due to the development of acidic conditions as a result of the accumulation of acidic hydrolysis products, as well as absorption of carbon dioxide from the atmosphere. The subsequent slow rate of degradation in distilled water is attributed to photochemical degradation. Photochemical degradation can be represented by the steps shown in Table 6. It can be shown that:

$$\frac{dP}{dt} = \left(\frac{k_p k_\phi}{k_{-\phi} + k_c + k_p} \right) [D]_t = k'_p [D]_t \qquad (2)$$

Table 6 Steps in the photolysis of dimethoate (D).

Step	Reaction	Rate constant	
1	$D + h\nu \rightarrow D^*$	k_ϕ	Light absorption
2	$D^* \rightarrow D + h\nu$	$k_{-\phi}$	Radiative relaxation
3	$D^* + M \rightarrow D + M^{\dagger}$	k_c	collisional relaxation
4	$D^* \rightarrow P$	k_P	Photolysis (P = products).

M = quencher molecule.

Equations 1 and 2 are in effect pseudo-first-order rate laws, in which $[D]_t = [D]_o - \Delta[D]$ = concentration of dimethoate at any time t in days, $[D]_o$ is the initial concentration, and $\Delta[D]$ is the change in the concentration at any given time t. When $[D]_o \gg \Delta[D]$, Eqs. 1 and 2 reduce to

$$\frac{dP}{dt} = k'_h [D]_o = k''_h \qquad (3)$$

and

$$\frac{dP}{dt} = k'_p [D]_o = k''_p \qquad (4)$$

Both are constant, consistent with the constant linear rates degradation of 0.694 μg mL^{-1} day^{-1} and 0.0388 μg mL^{-1} day^{-1} obtained for the initial fast and subsequent slow rates of degradation in distilled water as discussed above. In Eq. 2, k'_p is the apparent rate constant for photochemical degradation of dimethoate in distilled water. From Table 4, $[D]_{o(\text{distilled water})} = 15.2$ g 100 L^{-1}; and from Fig. 3A, $k'_p[D]_o = 0.0388$ μg mL^{-1} day^{-1}, hence $k'_p = 2.95 \times 10^{-9}$ s^{-1}. Similarly for hydrolysis, $k'_h[D]_o = 0.694$ μg mL^{-1} day^{-1}, hence $k'_h = 5.27 \times 10^{-8}$ s^{-1}. For the photolysis reaction

$$\frac{\Delta[D]}{[D]_o} = \left(\frac{0.0388}{15.23} \right) \left(\frac{\mu\text{g mL}^{-1}\text{ day}^{-1}}{\text{mg L}^{-1}} \right) = 2.55 \times 10^{-4}\ \text{d}^{-1} \qquad (5)$$

Similarly, for the hydrolysis reaction

$$\frac{\Delta[D]}{[D]_o} = \left(\frac{0.6937}{15.23} \right) \left(\frac{\mu\text{g mL}^{-1}\text{ day}^{-1}}{\text{mg L}^{-1}} \right) = 4.56 \times 10^{-3}\ \text{d}^{-1} \qquad (6)$$

Hence the assumption that $[D]_o \gg \Delta[D]$, is justified in both cases.

3.2. Rates of Degradation in the Water and Sediment Phases of Microcosm Experiment

From Fig. 3, it is apparent that the rates of degradation of dimethoate, both in water and sediment phases of the experiment, consist of an initially fast rate of degradation, followed by a slower rate. The rapid degradation in the water phase lasted for about 25 days. In the sediment phase, the rapid degradation lasted for about 9 days. The slower rate of degradation lasted up to the end of the experiment period in both phases. In addition, both the fast and the slower rates of degradation of dimethoate in the water phase, as well as the sediment phase, of the experiment are linear, pointing to steady-state kinetics, and hence microbial degradation, whereby the observed rates correspond to the plateau in the Michaelis-Menten curve.[15–18] Microbial degradation is consistent with the heavy green algal growth observed between day 6 and day 64 in the dam water plus sediment experiment. Linear rates for biodegradation were reported previously for glyphosate, endosulfan I, endosulfan II, fenamiphos, pirimiphos-methyl, chlorpyrifos and paraquat.[15–18,23] As indicated in Table 3, the fast linear rate and the slow linear rate of degradation in the water phase of the experiment, are attributed to degradation of free and colloidal particle adsorbed dimethoate, respectively.[15–17,23] The existence of free and particle bound insecticide in water samples was previously demonstrated by Lee and Skemitt using immunoanalysis.[24]

As noted in the Experimental section, 149.0 μg mL^{-1} dimethoate was charged into the experimental tank at the start of the experiment. This is equal to a total of 14.9 g dimethoate charged into the system. Table 4 shows that the total dimethoate detected by the experiment after 90 days amounts to 13.14 g. Thus, after 90 days only 1.76 g dimethoate remained in the experimental tank, mostly as colloidal particle adsorbed, partly in the water phase and partly in the sediment phase of the experiment.

The fast degradation speciation form in the sediment with a degradation rate of 107.9 μg g^{-1} day^{-1}, is attributed to dimethoate dissolved in pore water in the sediment. Considering the volume of the water phase and the mass of the sediment phase in the experimental set-up, data in Table 3 suggest that dimethoate is more soluble in pore water than in the bulk of the water phase above the sediment, which is unlikely. A plausible explanation for the apparent greater solubility of dimethoate in sediment pore water is that the dissolution of dimethoate in the pore water is enhanced by the existence of surface adsorption equilibria involving sediment particles, so that as degradation of free dimethoate in the pore water proceeds, the equilibrium shifts in favour of free dimethoate, thus:

$$\text{S-D} \rightleftharpoons \text{S} + \text{D} \qquad (7)$$

where S = surface adsorption site on sediment particle, and D = dimethoate molecule. As such surface complexes are essentially 1:1 (or monolayer) complexes, desorption is very fast, and the rate of degradation will be limited by the rate of microbial degradation of the free pesticide molecules in the pore water.

3.3. Proposed Microbial Degradation Kinetics Model

The degradation trends above are similar to those that have been reported for glyphosate, endosulfan I and endosulfan II, fenamiphos, pirimiphos-methyl and chlorpyrifos.[15–18] In terms of the speciation forms discussed above, data in Table 3 suggest that the degradation of dimethoate occurs according to the steps shown in Table 7.

Table 7 Microbial degradation of dimethoate, D, in the aquatic environment: Proposed kinetics model.

Step [a]	Water phase		Sediment phase	
	Reaction [b]	Rate constant	Reaction [b]	Rate constant
1(a)	$D + M \rightarrow D_B$ $D_B \rightarrow D + M$	k_1 k_{-1}	$D + M \rightarrow D_B$ $D_B \rightarrow D + M$	k_1 k_{-1}
2	$D_B + E \rightarrow DE$ $DE \rightarrow D_B + E$ $DE \rightarrow P + E$	k_2 k_{-2} k_3	$D_B + E \rightarrow DE$ $DE \rightarrow D_B + E$ $DE \rightarrow P + E$	k_2 k_{-2} k_3
1(b)	$D + nC_1 \rightarrow D(C_1)_n$ $D(C_1)_n \rightarrow D + nC_1$	k_4 k_{-4}	$D + mC_1 \rightarrow D(C_1)_m$ $D(C_1)_m \rightarrow D + mC_1$	k_4 k_{-4}
1(c)			$D + zS \rightarrow D(S)_z$ $D(S)_z \rightarrow D + zS$	k_5 k_{-5}

[a]Step 1(a) = Binding by microorganism; 2 = Binding and degradation by enzyme; 1(b) = Adsorption by colloidal particles; 1(c) = Adsorption by sediment particles.
[b]D = dimethoate; M = microorganism; DE = dimethoate-enzyme complex; E = enzyme; P = products; subscript B = 'microbial-bound'; C_1 = colloidal particle, type 1; DC = dimethoate-colloidal particle complex; S = sediment particle.

3.3.1. *Dimethoate Dissolved Fraction in the Water Phase and Sediment Pore Water*

From Steps 1(a) and 2 (in Table 7), assuming $[E] \gg [D_B]$, hence $[E] \approx 1$; $k_3 \gg k_2$, i.e. $[DE] \approx 0$, and [D] is in large excess of [M], i.e. $[D] = 1$, it can be shown that:

$$\frac{dP}{dt} = \left(\frac{k_1}{k_{-1} + k_2}\right)\left(\frac{k_2 k_3}{k_{-2} + k_3}\right)[M]_W \tag{8}$$

$$\frac{dP}{dt} = k_E\left(\frac{k_1}{k_{-1} + k_2}\right)[M]_W = k'_E[M]_W = k''_{E(W)} \tag{9}$$

where $k''_{E(W)}$ is the apparent linear rate of microbial degradation of the free pesticide in solution in the water phase of the experiment, assuming $[M]_W$ is constant. Similarly for microbial degradation of dimethoate in solution in sediment pore water, we have:

$$\frac{dP}{dt} = \left(\frac{k_1}{k_{-1} + k_2}\right)\left(\frac{k_2 k_3}{k_{-2} + k_3}\right)[M]_S \tag{10}$$

and

$$\frac{dP}{dt} = k_E\left(\frac{k_1}{k_{-1} + k_2}\right)[M]_S = k'_E[M]_S = k''_{E(S)} \tag{11}$$

where $k''_{E(S)}$ is the apparent linear rate of microbial degradation of the free pesticide in solution in the sediment pore water, assuming $[M]_S$ is constant.

3.3.2. *Colloidal Particle Adsorbed Fraction in Water Phase and Sediment Pore Water*

From Steps 1(b) and 2, assuming $[D] \gg [D_B]$, $k_3 \gg k_2$, i.e. $[DE] \approx 0$, $[D(C_1)_n]$ is in large excess of [M], i.e. $[D(C_1)_n] = 1$, and $[C_1]$ is constant and in large excess, it can be shown that:

$$\frac{dP}{dt} = \left(\frac{k_1}{k_{-1} + k_2}\right)\left(\frac{k_2 k_3}{k_{-2} + k_3}\right)\left(\frac{k_{-4}}{k_4}\right)[M]_W \tag{12}$$

$$\frac{dP}{dt} = k_{E(w)}\left(\frac{k_{-4}}{k_4}\right)[M]_W = k_{C1(w)}[M]_W = k'_{C1(W)} \tag{13}$$

where $k_{C1(W)}$ = rate constant for enzymatic degradation of colloidal particle adsorbed dimethoate in the water phase, and $k'_{C1(W)}$ is the linear rate of degradation of colloidal particle adsorbed dimethoate obtained experimentally. This occurs when $[M]_W$ is constant in Eq. 13.

Similarly, for colloidal particle adsorbed pesticide in the sediment:

$$\frac{dP}{dt} = \left(\frac{k_1}{k_{-1} + k_2}\right)\left(\frac{k_2 k_3}{k_{-2} + k_3}\right)\left(\frac{k_{-4}}{k_4}\right)[M]_S \tag{14}$$

$$\frac{dP}{dt} = k_{E(w)}\left(\frac{k_{-4}}{k_4}\right)[M]_S = k_{C1(S)}[M]_S = k'_{C1(S)} \tag{15}$$

where $k_{C1(S)}$ = rate constant for enzymatic degradation of colloidal particle adsorbed dimethoate in the sediment phase, and $k'_{C1(S)}$ is the linear rate of degradation of colloidal particle adsorbed dimethoate in the sediment obtained experimentally. This occurs when $[M]_S$ is constant in Eq. (15).

3.3.3. *Sediment Particle Adsorbed Fraction in Sediment Phase*

From Steps 1(c) and 2, assuming $[D] \gg [D_B]$, $k_3 \gg k_2$, i.e. $[DE] \approx 0$, $[D(S)_z]$ is in large excess of [M], i.e. $[D(S)_z] = 1$, and [S] is constant and in large excess, it can be shown that:

$$\frac{dP}{dt} = \left(\frac{k_1}{k_{-1} + k_2}\right)\left(\frac{k_2 k_3}{k_{-2} + k_3}\right)\left(\frac{k_{-5}}{k_5}\right)[M]_S \tag{16}$$

$$\frac{dP}{dt} = k_{E(w)}\left(\frac{k_{-5}}{k_5}\right)[M]_S = k_S[M]_S = k'_S \tag{17}$$

where k_S = rate constant for enzymatic degradation of sediment particle adsorbed dimethoate in the sediment phase, and k'_S is the corresponding linear rate of degradation of sediment particle adsorbed pesticide when $[M]_S$ is constant.

3.3.4. *Overall Rate of Degradation of Dimethoate in the Water Phase and in the Sediment Phase*

From Table 3, the overall rate of degradation in the water phase of the experiment is given by

$$\frac{dP}{dt} = (k'_h[D]_o) + (k'_P[D]_o) + k'_E[M]_{(W)} + k_{C_1}[M]_{(W)} \tag{18}$$

or

$$\frac{dP}{dt} = (k''_h) + (k''_P) + k''_{E(W)} + k'_{C_1(W)} \tag{19}$$

whereas the overall rate of degradation in the sediment phase of

the experiment is given by

$$\frac{dP}{dt} = k'_E[M]_{(S)} + \left(k_S[M]_{(S)}\right) + k_{C_1(S)}[M]_{(S)} \quad (20)$$

or

$$\frac{dP}{dt} = k''_{E(S)} + \left(k'_S\right) + k'_{C_1(S)} \quad (21)$$

In Eqs. 18, 19, 20 and 21 $k'_h[D]_o$, $k'_P[D]_o$, k''_h and k''_p are bracketed to signify that these steps are not observed in the aquatic microcosm experiment because the rate of microbial degradation is faster than the rate of hydrolysis and the rate of photochemical degradation, while $k'_S[M]_S$ and $k'_S[M]_S$ are bracketed to signify that this step is not observed in the aquatic microcosm experiment because the rate of desorption of the sediment particle adsorbed pesticide is faster than the rate of microbial degradation.

3.4. Possible Dimethoate Pollution Remediation Strategies

Equations 8, 10, 12, 14 and 16 define the factors that affect the rate of degradation of dimethoate in the aquatic environment. Any remediation measures for the abatement of dimethoate pollution of aquatic ecosystems must be designed to (a) maximize k_1, k_2, k_3, k_{-4}, k_{-5} and the density of microorganisms capable of degrading the pesticide, and (b) minimize k_4 and k_5, the rate constants for the adsorption of the pesticide by colloidal particles in the ecosystem. The rate constants k_1, k_2 and k_3 can be maximized by proper selection of the microorganism(s). Under such conditions, $k_3 \gg k_{-2}$ and $k_2 \gg k_{-1}$, and assuming C_1 and S are in large excess, Eqs. 12, 14 and 16 reduce to:

$$k''_{C_1(\max)} = k_1\left(\frac{k_{-4}}{k_4}\right)[M]_W = k_1\left(\frac{1}{K_4}\right)[M]_W \quad (22)$$

$$k''_{C_1(\max)} = k_1\left(\frac{k_{-4}}{k_4}\right)[M]_S = k_1\left(\frac{1}{K_4}\right)[M]_S \quad (23)$$

and

$$k''_{C_2(\max)} = k_1\left(\frac{k_{-5}}{k_5}\right)[M]_S = k_1\left(\frac{1}{K_5}\right)[M]_S \quad (24)$$

where K_4 and K_5 are the equilibrium constants for Step 1b and Step 1c respectively in Table 7. Several attempts have been made to find the optimum pH and temperature conditions and the best microorganisms for the bioremediation of aquatic systems polluted by dimethoate.[8,25,26] Equations 22 to 24 suggest that even after k_1, k_2, k_3 and [M] have been maximized, the rate of desorption of the pesticide can still be rate-limiting. The need to understand more fully the pesticide adsorption/desorption processes cannot therefore be over-emphasized.

3.5. Adsorption/Desorption by Colloidal Particles: Apparent Thermodynamic Properties

Assuming $[M]_W$ and $[M]_S$ are constant in Eqs. 8, 10, 12 and 14, we can equate Eqs. 8, 10, 12 and 14 to the linear rates of degradation represented by these equations, i.e. Eqs. 8, 10, 12 and 14 are equal to 3.12, 108, 0.358 and 1.03 μg g^{-1} day^{-1}, respectively. The adsorption/desorption equilibrium constants for the adsorption of dimethoate by colloidal particles in the water phase and sediment phase, $(k_4/k_{-4})_W$ and $(k_4/k_{-4})_S$, can be obtained by dividing Eq. 12 and Eq. 14 by Eq. 8 and Eq. 10, respectively. The values obtained are shown in Table 8. The free energy of activation for adsorption, $\Delta G_{(ads)}$, can be calculated from the relationship:[27,28a]

$$-RT\ln K_{ads} = \Delta G_{ads} \quad (25)$$

Values of ΔG_{ads} calculated for the dimethoate/colloidal-particle adsorption complexes in Table 3 are shown in Table 8. From the negative free energy of activation for adsorption, ΔG_{ads} in Table 8, it is apparent that the adsorption of dimethoate to type C_1 colloidal particles is thermodynamically favourable (negative ΔG).

Table 8 Adsorption/desorption of dimethoate by colloidal particles: apparent adsorption equilibrium constant (K_{ads}) and apparent adsorption free energy (ΔG_{ads}).

Adsorption complex	K_{ads}	ΔG_{ads} /J mol^{-1}
$D(C_1)_n$	8.71	–46 300
$D(C_1)_m$	105	–99 500

The entropy of activation, a measure of the difference in the disorderedness or randomness of the activated complex and the reactants, is given by:[27]

$$\Delta G^{\mp} = \Delta H^{\mp} - T\Delta S^{\mp} \quad (26)$$

For adsorption processes, the entropy of activation is a measure of the disorderness of the adsorption complex and reactants. As adsorption necessarily results in reduced disorder, the ΔS_{ads} for adsorption is necessarily negative. The negative values obtained for ΔG_{ads} in Table 8 can only be interpreted to mean that $\Delta H^{\ddagger}$ is negative and numerically greater than $T\Delta S^{\ddagger}$. In other words, the adsorption of dimethoate by colloidal particles is exothermic and is enthalpy-driven.[28b,29] According to Atkins, for physisorption, $\Delta H_{(P)}$ is rarely more negative than about –25 kJ mol^{-1}, whereas for chemisorption, $\Delta H_{(C)}$ is usually more negative, and sometimes much more negative, than –40 kj mol^{-1}. This leads us to conclude that the adsorption of dimethoate by colloidal particles both in the water phase and sediment phase, involves chemisorption, since $\Delta H \geq \Delta G$.

The values of $\Delta G^{\ddagger}$ in Table 8 suggest that the adsorption of dimethoate to type C_1 colloidal particles in the sediment involves a greater decrease in free energy than adsorption to colloidal particles of the same type in the water phase. The greater decrease in free energy when dimethoate adsorbs to colloidal particles in the sediment may be due to multiple colloidal particles adsorbed to a single dimethoate molecule as a result of the increased concentration of colloidal particles in the sediment, i.e. *m* greater than *n* in $D(C_1)_n$ and $D(C_1)_m$. Assuming $\Delta S = 0$ (i.e. equilibrium conditions), and that the value of –46.3 kj mol^{-1} for $\Delta H^{\ddagger}$ in the water phase corresponds to a single adsorption bond, i.e. $n = 1$, then the value of –99.5 kj mol^{-1} for $\Delta H^{\ddagger}$ in the sediment pore water phase corresponds to two adsorption bonds, i.e. $m = 2$. That is, the colloidal particle adsorption complexes have the structure D-C in the water phase, and C-D-C in the sediment phase. If we assume that microbial organisms will only bind free pesticide molecules,[24] then we should expect a slower degradation rate for colloidal-particle-dimethoate adsorption complex in the sediment phase.

3.6 Applicability of the Enzymatic Kinetics Model to other Pesticides

The pesticides that have so far been studied using the linear rate model approach include organophosphates (glyphosate, fenamiphos, chlorpyrifos and pirimiphos-methyl),[15,16] organochlorines (endosulfan I and II),[17] and the bipyrimidium herbicide, paraquat.[18] In all cases studied, biphasic linear degradation rates were observed for the water phase of the microcosm experiment. Biphasic linear degradation rates were also observed for the sediment phase, except for glyphosate for which a monophasic linear degradation rate was observed. From the pesticides studied so far, it appears that linear rates of degradation can

always be expected, provided the assumptions made in arriving at the enzymatic kinetics model above, are met. These are (a) the molecular number density (or concentration) of the pesticide is in excess of the microbial number density of the micro-organism(s) capable of binding and metabolizing the pesticide, and (b) the microbial number density is constant.[15] Microcosm experiments can be designed so that these assumptions are met. However, under real environmental conditions, assumption (b) is likely to be influenced by environmental factors such as availability of nutrients, pH and temperature. Sudden changes in these factors can lead to significant changes in microbial counts, and hence degradation rates. As long as linear rates are observed the kinetics model as presented in Table 7 will be applicable. Whether monophasic, biphasic or tri-phasic, etc., linear rates are observed, steps 1(c), 1(d), etc., can be removed or added as required. Poly-phasic linear rates can be expected where adsorption occurs on two or more different types of colloidal and/or sediment particles.

4. Conclusions

From the foregoing discussion, we conclude that dimethoate exists in solution as well as in three adsorption speciation forms in the aquatic environment. The adsorption forms consist of (a) a sediment particle physisorbed form, which is highly labile, and in equilibrium with dimethoate in solution in the sediment phase pore water; and (b) a slow degradation colloidal particle chemisorbed form, found in the water phase as well as the sediment phase. The degradation of all speciation forms proceeds *via* linear rates, and is primarily due to microbial decomposition.

Acknowledgements

This work was supported by a grant from the Research Board of the University of Zimbabwe. The support of one of us (J M.) by the Zimbabwe Tobacco Research Board is gratefully acknowledged. Our thanks are also due to Agricula (Pvt) Ltd for supplying the sample of Rogor used in the study.

References

1 W.J. Hayes and E.R. Laws, eds., *Handbook of Pesticide Toxicology*, vol. 3, Academic Press, San Diego, 1990.
2 US EPA, *Interim Re-registration Eligibility Decision for Dimethoate*. US EPA, Washington DC 20460, 2006.
3 G. Begum and S. Vijayaraghavan, *Bull. Environ. Contam. Toxicol.*, 1995, **54**, 370–375.
4 C.D.S. Tomlin, ed., *The Pesticide Manual*, 11th edn., British Crop Protection Council, Farnham, Surrey, UK, 1997.
5 S. Kumar and M. Singh, *J. Exp. Zool. India*, 2000, **3**(1), 83–88.
6 V.K. Srivastava and A. Singh, *Malay. Appl. Biol.*, 2001, **30**, 17–23.
7 Food and Agriculture Organization, Dimethoate FAO Evaluation Report 59/2001, in *FAO Specifications and Evaluations for Agricultural pesticides: Dimethoate* O,O-*dimethyl S-methyl carbamoylmethyl phosphorodithioate*. FAO, Rome, 2005, 12–22.
8 A. Abdel-Megeed and F.A.M. El-Nakieb, *Terrestrial and Aquatic Environmental Toxicology,* 2008, **2**(1), 1–4.
9 R.N. Singh, R.K. Pandey, N.N. Singh and V.K. Das, *World J. Zoology*, 2009, **4**(2), 70–75.
10 R.K. Pandey, R.N.Singh, S. Singh, N.N. Singh, and V.K. Das, *J. Environ. Biol.*, 2009; **30**(3), 437–440.
11 W. Heger, S.T. Jung, S. Martin, and H. Peter, *Chemosphere*, 1995, **31**, 2707–2726.
12 World Health Organization (WHO). Organophosphorus pesticides, a general introduction, in *Environmental Health Criteria 63 Special Report*, WHO, Geneva, 1986.
13 W.R. Bohn, *J. Economic Entomology*, 1964, **57**(6), 798–799.
14 B.L. Parker and J.E. Dewey, *J. Economic Entomol.*, 1965; **58**(1), 106–111.
15 M.F. Zaranyika and M.G. Nyandoro, *J. Agri. Food Chem.*, 1993; **41**(5), 838–842.
16 M.F. Zaranyika, M. Jovani and J. Jiri, *S.A. J. Chem*. 2010, **63**, 227–232.
17 M.F. Zaranyika and J. Mlilo, Degradation of fenamiphos, chlorpyrifos and pirimiphos-methyl in the aquatic environment: a proposed enzymatic kinetic model that takes into account adsorption/desorption of the pesticide by colloidal and sediment particles, in *Pesticides Recent Trends in Pesticide Assay*, (R.P. Soundararajan, ed.), InTech Publishers, Croatia, 2012, 193–216.
18 M.F. Zaranyika and S. Nyoni, *Intern. J. Res. Chem. Environ. (IJRCE)*, 2013; **3**(3), 26–35.
19 M. Mansour, K. Hustert and R. Muller, *Intern. J. Environ. Anal. Chem.*, 1989; **37**(2), 83–90.
20 P.A. Greve and C.C. Goewie, *Intern. J. Environ. Anal. Chem.*, 1985; **20**, 29–39.
21 H. Tse, M. Comba and M. Alaee, *Chemosphere*, 2004, **54**(1), 41–47.
22 P.A. Giang and M.S. Schechter, *J. Agric. Food Chem.*, 1963, **11**(1), 63–66.
23 N.S. Nomura and H.W. Hilton, *Weed Res.*, 1977, **17**, 113–121.
24 N. Lee and J.H. Skemitt, *Food and Agricultural Immunology*, 1998, **10**(1), 3–12.
25 Y. Liu, Y. Chung and Y. Xiong, *Appl. Environ. Micobiol.*, 2001, **67**, 3746–3749.
26 M. DebMandal, S. Mandal and N.K. Pal, *Indian Res. J. Chem. Environ.*, 2002, **6**, 49–62
27 R.E. Weston, Jr and H.A. Schwarz, *Chemical Kinetics.* Prentice-Hall, Eaglewood Cliffs, New Jersey, USA, 1972, pp. 108–109.
28 P.W. Atkins, Physical *Chemistry*, Oxford University Press, UK, 1978, (a) p. 913, (b) p. 938.
29 G.W. Castellan, *Physical Chemistry*, 2nd edn., Addison-Wesley, Massachusetts, 1971, p. 785.
30 M.F. Zaranyika and N.T. Mandizha, *J. Environ. Sci. Health Part B*, 1998, **33**(3), 235–251.